High-Power and High-Linearity Photodetector Modules for Microwave Photonic Applications

Efthymios Rouvalis, *Member, IEEE*, Frederick N. Baynes, Xiaojun Xie, Kejia Li, Qiugui Zhou, Franklyn Quinlan, Tara M. Fortier, Scott A. Diddams, *Fellow, OSA*, Andreas G. Steffan, Andreas Beling, *Fellow, OSA*, and Joe C. Campbell, *Fellow, IEEE*

***Abstract*—We demonstrate hermetically packaged InGaAs/InP photodetector modules for high performance microwave photonic applications. The devices employ an advanced photodiode epitaxial layer known as the modified uni-traveling carrier photodiode (MUTC-PD) with superior performance in terms of output power and saturation. To further improve the thermal limitations, the MUTC-PDs were flip-chip bonded on high thermal conductivity substrates such as Aluminum Nitride (AlN) and Diamond. Modules using chips with active area diameters of 40, 28, and 20 μm were developed. The modules demonstrated a 3-dB bandwidth ranging from 17 GHz up to 30 GHz. In continuous wave mode of operation, very high RF output power was achieved with 25 dBm at 10 GHz, 22 dBm at 20 GHz, and 17 dBm at 30 GHz. In addition, the linearity of the modules was characterized by using the third order intercept point (OIP3) as a figure of merit. Very high values of OIP3 were obtained with 30 dBm at 10 GHz, 25 dBm at 20 GHz and more than 20 dBm at 30 GHz. Under short pulse illumination conditions and by selectively filtering the 10 GHz frequency component only, a saturated power of $>$21 dBm was also measured. A very low AM-to-PM conversion coefficient was measured, making the modules highly suitable for integration in photonic systems for ultralow phase noise RF signal generation.**

***Index Terms*—1-dB compression, Analog photonic links, high-power photodetectors, millimeter-wave source, modified uni-traveling carrier photodiode (MUTC-PD), third-order intermodulation distortion (IMD3).**

I. Introduction

IT has been shown that high-power, high-linearity photodiodes provide significant advantages in many analog photonic applications including analog optical links [1], antenna transmit and receive applications [2], and photonic microwave generation [3]. In these systems the photodiode (PD) must be able to deliver very high photocurrent level and, thus, high RF output power, to improve link gain and SNR, while maintaining high linearity. Several photodiode structures including the uni-traveling carrier (UTC) PD [4], the partially-depleted-absorber PD [5], and the modified UTC (MUTC) PD [6] have been developed to alleviate the space-charge screening effect that limits the high-power capability. Through uniform absorber illumination [7], and the use of substrates with high thermal conductivity [8] RF output power levels have been further improved. Although significant previous work on high-power photodetector chip technology has been published, only a limited number of module demonstrations have been reported so far. Demonstrations of packaged modules based on a partially-depleted-absorber chip design reported high power levels of up to 25 dBm at 5 GHz in a TO-can package [9] and 29 dBm at 5 GHz in a butterfly package using an array of 8 PDs and a Wilkinson RF power combiner [10]. However, in [9] the 3-dB bandwidth of the modules was limited only to 8 GHz.

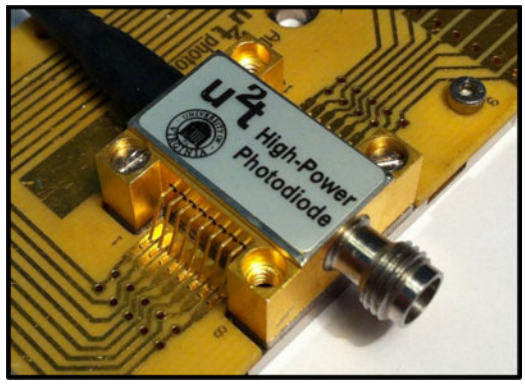

Fig. 1. Image of the packaged high power photodetector module with high-frequency RF interface.

In this paper, we demonstrate fully-packaged photodetector modules based on an MUTC-PD design with a 3-dB bandwidth of up to 30 GHz. An image of the packaged module is shown in Fig. 1. The modules achieved record-high output power levels of up to 25 dBm at 10 GHz, 22 dBm at 22 GHz, and 17 dBm at 30 GHz. In addition, highly linear performance was achieved up to very high photocurrent levels. An output third order intercept point (OIP3) ranging from 30 dBm at 10 GHz to 20 dBm at 30 GHz was measured. Very high output power was also measured in pulsed mode operation together with low values of AM-to-PM conversion coefficient. Therefore, these

Manuscript received January 14, 2014; revised February 20, 2014; accepted February 22, 2014. Date of publication March 10, 2014; date of current version September 1, 2014. This work was supported in part by the Naval Research Laboratory (NRL) and the DARPA PULSE program.

E. Rouvalis and A. G. Steffan are with the u^{2}t Photonics AG, Berlin 10553, Germany (e-mail: rouvalis@u2t.de; steffan@u2 t.de).

X. Xie, K. Li, Q. Zhou, A. Beling, and J. C. Campbell are with the Department of Electrical and Computer Engineering, University of Virginia, Charlottesville, VA 22904 USA (e-mail: xx5 wr@virginia.edu; kl7 pb@virginia.edu; qz6 s@virginia.edu; ab3pj@virginia.edu; jcc7 s@virginia.edu).

F. N. Baynes, F. Quinlan, T. M. Fortier, and S. A. Diddams are with the National Institute of Standards and Technology, Boulder, CO 80305 USA (e-mail: frederick.baynes@nist.gov; franklyn.quinlan@nist.gov; tara.fortier@nist.gov; scott.diddams@nist.gov).

Color versions of one or more of the figures in this paper are available online at http://ieeexplore.ieee.org.

Digital Object Identifier 10.1109/JLT.2014.2310252

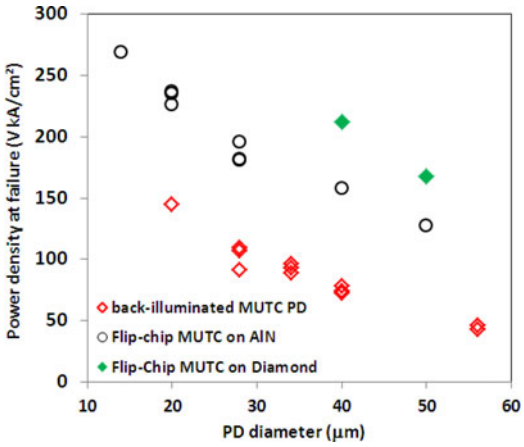

Fig. 2. DC power at the point of failure defined as the product of the reverse bias and the average photocurrent normalized to PD area.

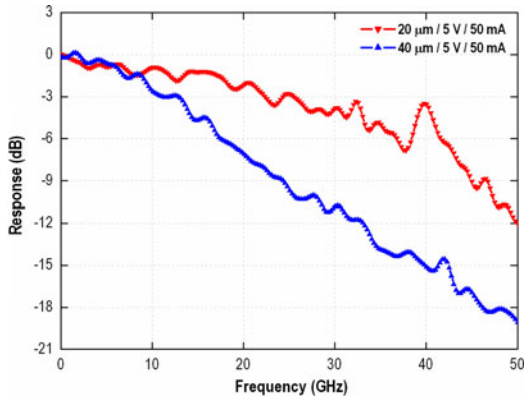

Fig. 3. Frequency response measurements using an LCA of two packaged high power photodetector modules with 40 μm active area diameter (blue, triangles) and 20 μm active area diameter (red, inverse triangles).

photodetector modules can be key components for a wide range of microwave photonic systems.

II. Photodiode Chip Design

The photodiode epitaxial layer stack corresponds to a charge compensated MUTC-PD with both absorbing and non-absorbing depleted regions as described in [11]. The InGaAs absorber region with a thickness of 850 nm is comprised of a 150 nm n^- layer and four step-graded p-doped layers ranging from 5×10^{17} to 2×10^{18} cm^{-3}. The 900 nm InP electron drift layer is slightly n-type doped for space charge compensation. Thin bandgap-graded InGaAsP layers are used to smooth the abrupt band barrier at the InGaAs–InP heterojunction interface. The structure also incorporates a 50 nm moderately n-type doped InP cliff layer to maintain high electric field at the absorber-drift layer interface. Back-illuminated mesa structures with diameters ranging between 14 μm and 56 μm were fabricated using standard microfabrication technologies [11]. Typical measured dark currents and responsivities at 1550 nm were 20 nA at 5 V and 0.7 A/W, respectively.

It has been previously shown that these MUTC-PDs with cliff layer have mitigated the space-charge effect to the extent that thermal management has become the primary determining factor for high-power operation [12]. To improve thermal dissipation MUTC-PDs were flip-chip bonded to high-thermal conductivity submounts using an Au-Au thermo-compression bonding process. As shown in Fig. 2, the maximum dissipated power density of the photodiodes was increased by 65% to 90% as the result of flip-chip bonding on AlN substrate. Even higher values can be obtained when using diamond substrates. It is worth mentioning that smaller PDs sustain larger power densities; a fact that indicates the presence of a lateral component in the heat transport. It implies that the maximum available output power does not strictly scale with PD area which may benefit high-speed PDs. A flip-chip bonded 50 μm-diameter PD on AlN demonstrated a 1-dB compression current of 230 mA and maximum output power of 30 dBm at 10 GHz and 11 V reverse bias voltage. For a 40-μm-diameter PD a saturation current $>$180 mA was measured; the maximum RF output power was 28.8 dBm at 15 GHz. Since these photodiodes can be operated at a high reverse bias, the minimum OIP3 was larger than 47 dBm in the range of 40 to 160 mA at 300 MHz and remained above 30 dBm up to average photocurrents of 170 mA at 15 GHz [12].

III. Module Bandwidth and RF Saturation

The MUTC-PD chips were packaged hermetically with an SMF interface for efficient light coupling and an RF connector suitable for high frequency operation up to 67 GHz. An external bias-tee was used for all measurements reported here, while in order to obtain the maximum output power from the module, no impedance matching network was included in the package. Two types of chips were packaged with the reported technique. The first type included PD chips with a 40-μm active area diameter flip-chip bonded on an AlN substrate while the second type included chips with 40, 28, and 20 μm active area diameters on a diamond substrate. Inside the package, a thermoelectric cooler was placed in order to allow for thermally stable operation and efficient heat dissipation. All module measurements reported here were taken at a stabilized temperature of 15 °C, as provided by the thermistor reading. The constant temperature level provided a reference for stable and repeatable results. A 45° angle-cleaved SMF was used to couple light into the back-illuminated MUTC-PD through the anti-reflection coated substrate. To achieve the highest linearity and the best power saturation performance, the modules were coupled at a responsivity of 0.4 A/W at 1550 nm which was approximately 60% of the maximum achievable value (0.7 A/W).

Initially, the frequency response of the modules was measured up to 50 GHz with a calibrated Lightwave Component Analyzer (LCA). In order to measure the frequency response of the modules, appropriate light amplification was applied to the optical signal from the LCA. Measurements were taken from two modules, one with a 40 μm active area diameter on an AlN substrate and one with a 20 μm active area diameter on diamond. The results obtained at a dc photocurrent of 50 mA and reverse bias voltage of 5 V are shown in Fig. 3. In good agreement with chip-based measurements, 3-dB bandwidths of 23 and 13 GHz were measured for the modules with 20 and

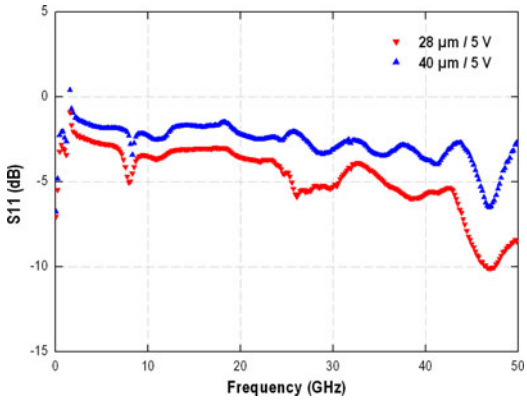

Fig. 4. S11 (RF return loss) of two packaged high power photodetector modules with 40 μm active area diameter (blue, triangles) and 28 μm active area diameter (red, inverse triangles).

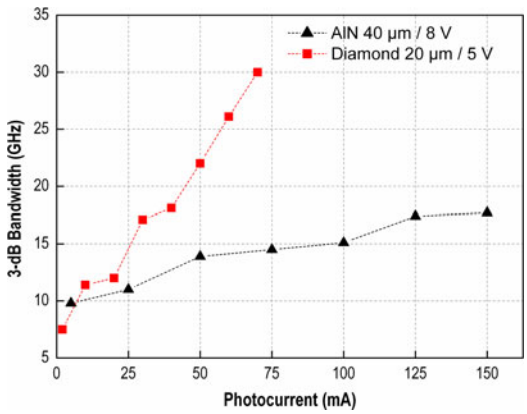

Fig. 5. Variation of 3-dB bandwidth as a function of module with a 40 μm diameter PD (black triangles) and a 20 μm PD (red squares).

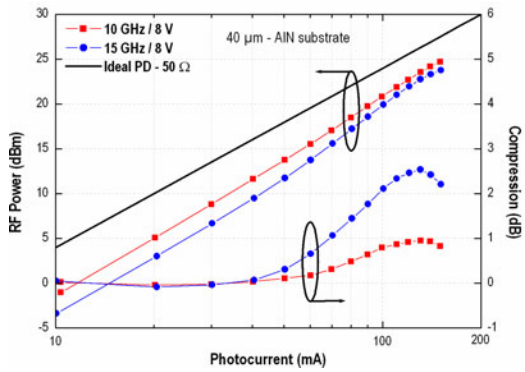

Fig. 6. Output RF power (left y-axis) in dBm and power compression (right y-axis) as a function of the dc photocurrent for a module using a 40 μm active area diameter MUTC-PD chip at 10 GHz (red squares) and 15 GHz (blue circles).

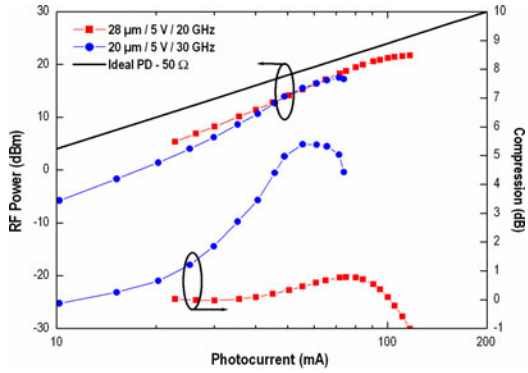

Fig. 7. Output RF power (left y-axis) in dBm and power compression (right y axis) as a function of the dc photocurrent for a module using a 28 μm active area diameter MUTC-PD chip at 20 GHz (red squares) and a module using a 20 μm active area diameter MUTC-PD Chip at 30 GHz (blue circles).

40 μm active area PD chips, respectively. The RF return loss (S11) was also measured using the same instrument for two modules without any impedance matching network and the results are plotted in Fig. 4. As a next step, the 3-dB bandwidth dependence with the respect to the DC photocurrent at a constant bias level was measured for these two modules and the results are shown in Fig. 5. A photocurrent-dependent 3-dB bandwidth was observed especially for the devices with the smaller active area diameter (20 μm), ranging from below 10 GHz at a photocurrent of $<$10 mA to 30 GHz at the maximum measurement photocurrent of 70 mA. The fact that both modules demonstrate a similar bandwidth at photocurrents below 25 mA indicates that at these photocurrent levels the response is transit-time limited and dominated by the electron diffusion time. This behavior is attributed to the self-biasing effect in the absorber of the MUTC-PD and has also been reported in other publications reporting photodiode chips with a UTC-PD or an MUTC-PD epitaxial structure [13]–[15].

The RF output power of the modules was measured at frequencies up to 30 GHz using an automated optical heterodyne system. The measurement system consists of two tunable lasers, polarization controllers, a high power EDFA and a calibrated RF power meter. The results for a packaged module using a PD with an active area diameter of 40 μm flip-chip bonded on AlN are shown in Fig. 6. The module demonstrated extremely high output RF power levels with 25 dBm at 10 GHz and 24 dBm at 15 GHz at a reverse bias voltage of 8 V and a maximum DC photocurrent of 150 mA. It is also noteworthy that this measurement was limited by the available output optical power from the EDFA and that the device remains below the 1-dB compression point up to 150 mA for these frequencies. By defining the power conversion efficiency (PCE) as the ratio of the output RF power to the total electrical dissipated power, PCE values of 26% at 10 GHz and 21% at 15 GHz are calculated. PCEs of even up to 53.5% have also been reported in [16] but at much lower frequencies ($<$1 GHz).

The second type of modules using 28 and 20 μm active area diameter PD chips flip-chip bonded on a diamond substrate and the same packaging configuration was also measured using the same heterodyne system and the results are shown in Fig. 7. In this case, output power levels of 22 dBm at 20 GHz and 17 dBm at 30 GHz at a reverse bias voltage of only 5 V were achieved from the 28 μm and the 20 μm devices, respectively. The corresponding photocurrents at which the 1-dB compression occurs were 105 mA (28 μm, 20 GHz) and 74 mA (20 μm, 30 GHz).

No significant difference in the RF-saturation performance was observed between modules using 40 μm chips with two different substrates. For example, the 1-dB compression currents

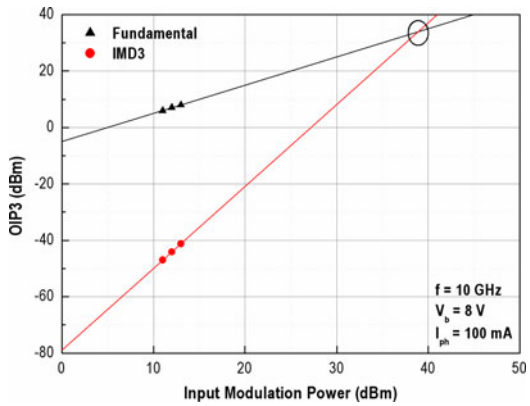

Fig. 8. Output third order intercept point measurement at 10 GHz at a reverse bias voltage of 8 V and a 100 mA photocurrent for a module with a 40-μm diameter PD.

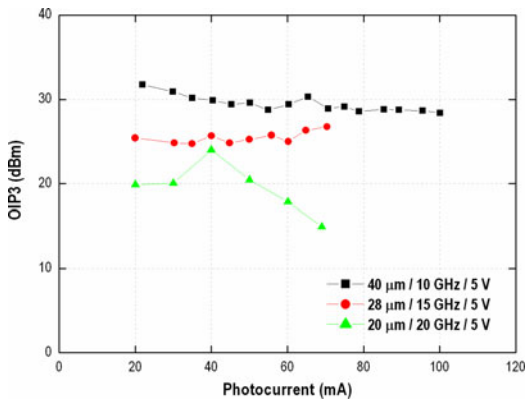

Fig. 9. OIP3 measurement as a function of the dc photocurrent at 10, 15, and 20 for PDs with active area diameters of 40, 28, and 20 μm, respectively. All measurements were taken at a reverse bias of 5 V.

at a frequency of 15 GHz for the same bias voltage (5 V) were found to be 143 and 146 mA for modules using Chips with AlN and Diamond substrates, respectively. This small difference can be attributed to the fact that both modules were operated far from the power density dissipation point of failure and thermal effects seemed to play no significant role in this.

IV. Linearity Measurements

The OIP3 of the packaged modules was characterized using a two tone experimental setup, similar to the ones reported in [17], [18]. The laser spectral spacing was kept large enough (150 GHz) to avoid any possible interference with the heterodyne signal. The two synthesizers used to produce the fundamental tones were synchronized and an offset of 10 MHz was used between the two tones. The two tones were combined and amplified and the resulting RF signals were measured using a 50 GHz Electrical Spectrum Analyzer, which was also synchronized with the synthesizers. For the module using the PD with a 40 μm active area diameter the OIP3 at 10 GHz was measured up to 100 mA. The experimental results at a dc photocurrent of 100 mA, reverse bias voltage of 8 V and a fundamental tone frequency of 10 GHz are plotted in Fig. 8. The calculated OIP3 was found to be 32.5 dBm.

As a next step, the OIP3 of modules with chips with 40, 28, and 20 μm was measured with respect to the DC photocurrent at frequencies of 10, 15, and 20 GHz, respectively. Fig. 9 shows the results of these measurements for the three different modules at a reverse bias voltage of 5 V. In the linear region of operation of the modules the corresponding OIP3 values were found to be in the order of 30 dBm at 10 GHz, 25 dBm at 15 GHz, and 20 dBm at 20 GHz.

V. Applications

The generation and dissemination of low noise microwave signals has applications in radar, high-speed signal processing, and time and frequency transfer. Optical frequency division, where a stable optical frequency is coherently divided to the microwave domain by an optical frequency comb, has recently emerged as a technique to generate microwave signals with

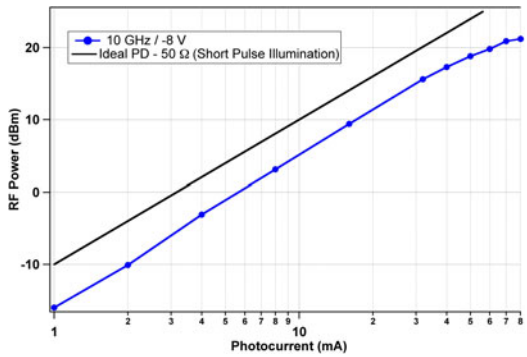

Fig. 10. Saturation of the output power of a packaged MUTC photodiode under short pulse (<10 ps) illumination used for optical frequency division. The ideal photodiode curve differs from the case of continuous sine-wave modulation shown in the other graphs by 6 dB.

extremely high spectral purity [19]. By photodetecting the optical pulse train of the frequency comb, 10 GHz signals have been produced with absolute phase noise below –100 dBc/Hz at 1 Hz offset, and nearly –180 dBc/Hz at 1 MHz offset. Such low noise places stringent demands on the power handling, noise, and linearity of the photodetection process under ultrashort optical pulse illumination. Here we discuss the saturation and linearity characteristics of a packaged 40 μm MUTC-PD flip-chip bonded on AlN heatsink when illuminated by picosecond optical pulses from an erbium fiber-based frequency comb.

With sufficiently low phase-noise, fundamental thermal noise can be a limiting factor in performance. Thus to improve the thermal noise limit, higher output microwave power is required. The microwave power saturation behavior of a photodiode under short-pulse (<10 ps) illumination differs from sine-wave illumination of the photodiode, reaching saturation at much lower microwave powers [20]. This problem is exacerbated when the optical pulse repetition rate is much lower than the microwave frequency to be generated. To counteract this effect, the 208.33 MHz repetition rate from our erbium fiber mode-locked laser was multiplied via pulse interleaving in a series of delay-line interferometers with half-period delays [21]. This resulted in a saturation power over 21 dBm at 10 GHz, shown in Fig. 10 for the packaged MUTC-PD at a reverse bias of 8 V.

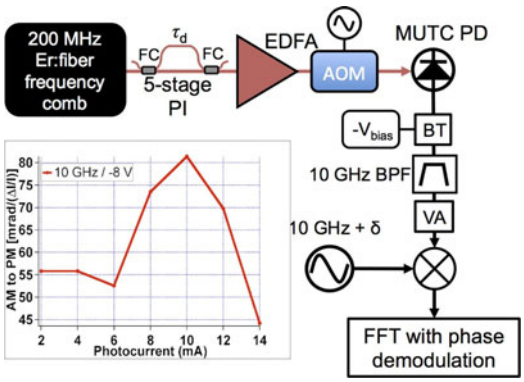

Fig. 11. Short pulse AM-to-PM measurement. Only one stage of the 5-stage pulse interleaver is represented. PI, pulse interleaver; EDFA, erbium-doped fiber amplifier; AOM, acousto-optic modulator; BT, bias tee; BPF, 10 GHz bandpass filter; VA, variable attenuator; FFT, fast Fourier transform spectrum analyzer. Inset: The AM-to-PM conversion factor for the packaged MUTC photodiode.

It should be noted the ideal photodiode curve in Fig. 10 differs from the case of sine-wave illumination by 6 dB due to the nature of short pulse illumination [22]. This is one of the highest reported 10 GHz power levels under short pulse illumination, for microwave power >20 dBm, the thermal noise-limited phase noise floor is <–197 dBc/Hz, and offers the potential for significant improvement in the microwave phase stability. However the phase noise floor may be limited by laser intensity noise coupled to microwave phase noise through amplitude-to-phase conversion in the photodiode, as outlined below.

In addition to high power, high linearity impacts the phase noise of the generated microwave signals. Whereas OIP3 is commonly used to assess the linearity of photodetectors in photonic links, here the appropriate measure of linearity is amplitude-to-phase (AM-to-PM) conversion. AM-to-PM conversion limits the phase stability of the generated microwave signals by coupling the optical pulse intensity fluctuations to phase fluctuations of the generated microwave [23], [24]. The setup used to quantify the AM-to-PM in the MUTC photodiode is shown in Fig. 11. The interleaved output of the erbium fiber laser was optically amplified and an acousto-optic modulator was used to amplitude modulate the optical pulse train at a frequency ω_{AM}. The resulting 10 GHz signal from the MUTC photodiodes was band-pass filtered and mixed with another signal at frequency $(10 + \delta)$ GHz to generate a signal at frequency δ (< 5 MHz). This signal was then phase-demodulated in an FFT analyzer. The AM-to-PM in the photodiode converts the AM tone at ω_{AM} to PM at the same frequency, the strength of which is normalized to the fractional amplitude variation of the optical pulse train to calculate the AM-to-PM conversion factor.

The resulting phase modulation on the photo-detected microwave signal was measured for different photocurrents at a constant temperature of 15 °C. Results of the AM-to-PM measurement for the packaged MUTC-PD are shown as the inset in Fig. 11 for low photocurrent. The MUTC-PD retains a high level of linearity without sacrificing output power. The presence of AM-to-PM conversion minima indicates the preferred photo-current at which to operate the device, and previous measurements show repeated minima at higher photocurrents [25]. By operating the photo-diode in one of the AM-to-PM conversion minima, contribution of laser intensity noise to the phase noise can be reduced by up to 30 dB, enabling exceptionally low phase noise microwave signals.

VI. Conclusion

Hermetically packaged photodetector modules suitable for microwave photonic applications are demonstrated. The modules employ flip-chip bonded MUTC-PD chips on high-thermal conductivity substrates, suitable for extremely high current operation. The modules exhibit very high output power levels together with very high OIP3 values. The excellent saturation power behavior measured in continuous wave mode is also maintained under short optical pulse excitation with highly stable fiber lasers. These features make our photodetector modules highly suitable not only for high performance analog photonic links, but also for use in photonic ultralow phase noise RF generation systems.

References

[1] V. J. Urick, F. Bucholtz, J. D. McKinney, P. S. Devgen, A. L. Campillo, J. L. Dexter, and K. J. Williams, "Long-haul analog photonics," *J. Lightw. Technol*, vol. 29, no. 8, pp. 1182–1205, 2011.

[2] R. Esman, S. Pappert, B. Krantz, and G. Gopalakrishnan, "Photonics for microwave generation, transmission and processing," in *Proc. Tech. Dig. Opt. Fiber Commun.*, 2009, paper OTuE5.

[3] T. M. Fortier, F. Quinlan, A. Hati, C. Nelson, J. A. Taylor, Y. Fu, J. C. Campbell, and S. A. Diddams, "Photonic microwave generation with high-power photodiodes," *Opt. Lett.*, vol. 38, pp. 1712–1714, 2013.

[4] N. Shimizu, Y. Miyamoto, A. Hirano, K. Sato, and I. Ishibashi, "RF saturation mechanism of In/InGaAs uni-travelling-carrier photodiode," *Electron. Lett.*, vol. 36, no. 8, pp. 750–751, Apr. 2000.

[5] X. Li, S. Demiguel, N. Li, J. C. Campbell, D. L. Tulchinsky, and K. J. Williams, "Backside illuminated high saturation current partially depleted absorber photodetectors," *Electron. Lett.*, vol. 39, no. 20, Oct. 2003.

[6] X. Wang, N. Duan, H. Chen, and J. C. Campbell, "InGaAs–InP photodiodes with high responsivity and high saturation power," *IEEE Photon. Technol. Lett.*, vol. 19, no. 16, pp. 1272–1274, Sep. 2007.

[7] A. Joshi and D. Becker, "GRIN lens-coupled top-illuminated photodetectors for high-power applications," in *Proc. IEEE Int. Top. Meet. Microw. Photon.,*, Oct. 3–5, 2007, pp. 18–20.

[8] N. Li, H. Chen, N. Duan, M. Liu, S. Demiguel, R. Sidhu, A. L. Holmes, and J. C. Campbell, "High power photodiode wafer bonded to Si using Au with improved responsivity and output power," *IEEE Photon. Technol. Lett.*, vol. 18, no. 23, pp. 2526–2528, Dec. 2006.

[9] K. Sakai, S. Itakura, M. Nakaji, E. Ishimura, and T. Aoyagi, "Coaxial high-current photodiode module for analog optical links," in *Proc. IEEE Photon. Conf.*, 2010, pp. 24–25.

[10] S. Itakura, K. Sakai, T. Nagatsuka, E. Ishimura, M. Nakaji, H. Otsuka, K. Mori, and Y. Hirano, "High-current backside-illuminated photodiode array module for optical analog links," *J. Lightw. Technol.*, vol. 28, no. 6, pp. 965–971, 2010.

[11] Z. Li, H. Pan, H. Chen, A. Beling, and J. C. Campbell, "High saturation current modified uni-traveling-carrier photodiode with cliff layer," *IEEE J. Quantum Electron.*, vol. 46, no. 5, pp. 626–632, May 2010.

[12] Z. Li, Y. Fu, M. Piels, H. Pan, A. Beling, J. E. Bowers, and J. C. Campbell, "High-power high-linearity flip-chip bonded modified uni-traveling carrier photodiode," *Opt. Exp.*, vol. 19, no. 26, pp. B385–B390, 2011.

[13] H. Pan, Z. Li, A. Beling, and J. C. Campbell, "Characterization of high-linearity modified uni-traveling carrier photodiodes using three-tone and bias modulation techniques," *J. Lightw. Technol.*, vol. 28, no. 9, pp. 1316–1322, 2010.

[14] M. Chtioui, F. Lelarge, A. Enard, F. Pommereau, D. Carpentier, A. Marceaux, F. Van Dijk, and M. Achouche, "High responsivity and high power UTC and MUTC GaInAs-InP photodiodes," *IEEE Photon. Technol. Lett.*, vol. 24, no. 4, pp. 318–320, Feb. 2012.

[15] H. Ito, S. Kodama, Y. Muramoto, T. Furuta, T. Nagatsuma, and T. Ishibashi, "High-speed and high-output InP-InGaAs unitraveling-carrier photodiodes," *IEEE J. Sel. Topics Quantum Electron.*, vol. 10, no. 4, pp. 709–727, Jul. 2004.
[16] U. Gliese, K. Colladay, A. S. Hastings, D. A. Tulchinsky, V. J. Urick, and K. J. Williams, "53.5% Photodiode RF power conversion efficiency," in *Proc. Opt. Fiber Commun.*, San Diego, CA, USA, Mar. 2010, PDP A7.
[17] E. Rouvalis, Q. Zhou, A. Beling, A. S. Cross, A. G. Steffan, and J. C. Campbell, "High- power and high-linearity photodetector module based on a modified uni-traveling carrier photodiode," in *Proc. IEEE Int. Top. Meet. Microw. Photon.*, 2013, pp. 13–16.
[18] H. Jiang, D. S. Shin, G. L. Li, T. A. Vang, D. C. Scott, and P. K. L. Yu, "The frequency behavior of the third-order intercept point in a waveguide photodiode," *IEEE Photon. Technol. Lett.*, vol. 12, no. 5, pp. 540–542, May 2000.
[19] T. Fortier, M. Kirchner, F. Quinlan, J. Taylor, J. Bergquist, T. Rosebland, N. Lemke, A. Ludlow, Y. Jiang, C. Oates, and S. Diddams, "Generation of ultrastable microwaves via optical frequency division," *Nature Photon.*, vol. 5, pp. 425–429, 2011.
[20] S. Diddams, M. Kirchner, T. Fortier, D. Braje, A Wiener, and L. Hollberg, "Improved signal-to-noise ratio of 10 GHz microwave signals generated with a mode-filtered femtosecond laser frequency comb," *Opt. Exp.*, vol. 17, pp. 3331–3340, 2009.
[21] A. Haboucha, W. Zhang, T. Li, M. Lours, A. Luiten, Y. Le Coq, and G. Santarelli, "Optical-fiber pulse rate multiplier for ultralow phase-noise signal generation," *Opt. Lett.*, vol. 36, pp. 3654–3656, 2011.
[22] R. Scott, C. Langrock, and B. Kolner, "High dynamic-range laser amplitude and phase noise measurement techniques," *IEEE J. Sel. Topics Quantum Electron.*, vol. 7, no. 4, pp. 641–655, Jul./Aug. 2001.
[23] J. Taylor, S. Datta, A. Hati, C. Nelson, F. Quinlan, A. Joshi, and S. Diddams, "Characterisation of power-to-phase conversion in high-speed P-I-N photodiodes," *IEEE Photon. J.*, vol. 3, no. 1, pp. 140–151, Feb. 2011.
[24] W. Zhang, T. Li, M. Lours, S. Seidelin, G. Santarelli, and Y. Le Coq, "Amplitude to phase conversion of InGaAs pin photo-diodes for femtosecond lasers microwave signal generation," *Appl. Phys. B*, vol. 106, no. 2, pp. 301–308, 2012.
[25] T. Fortier, F. Quinlan, A. Hati, C. Nelson, J. Taylor, Y. Fu, J. Campbell, and S. Diddams, "Photonic microwave generation with high-power photodiodes," *Opt. Lett.*, vol. 38, pp. 1712–1714, 2013.

Efthymios Rouvalis received the Dipl. Ing. degree from the National Technical University of Athens, Greece, in 2007, and the Ph.D. degree in electrical engineering from University College London, U.K., in 2011. After the completion of his doctoral studies at University College London he was awarded a one-year EPSRC doctoral prize fellowship in 2011 to work on applications of high speed InP photodetectors in Terahertz spectroscopic systems. Since 2012, he has been with u^2t Photonics AG. His research interests include optoelectronic devices for high speed optical communications and microwave photonic applications with particular emphasis on mode-locked lasers, high power photodetectors, photonic integration, high speed coherent photodetectors, and InP modulators. He has authored and coauthored more than 30 technical papers in international conferences and journals. He regularly acts as a Reviewer for several IEEE and OSA publications.

Frederick N. Baynes received the Ph.D. degree from the University of Western Australia in 2012 for an optical resonator-based test of Lorentz Invariance. He is currently undertaking a postdoctoral position at the National Institute of Standards and Technology in Boulder, Colorado, working on the generation of ultra-low phase noise microwaves through optical frequency division.

Xiaojun Xie received the B.S. degree in optoelectronic technology from the University of Electronic Science and Technology of China, Chengdu, China, in 2010, and the M.S. degree in electronic science and technology from Beijing University of Posts and Telecommunications, Beijing, China, in 2013. He is currently working toward the Ph.D. degree in electrical engineering at the University of Virginia, VA, USA. His current research interests include high power, high bandwidth and high linearity photodiodes, waveguide photodiodes and microwave photonics.

Kejia Li was born in Tianjin, China. She received the M.S. degree in electrical engineering from Peking University Beijing, China, in 2008 and the Ph.D. degree in electrical engineering from University of Virginia, VA, USA, in 2012. She is currently a Research Scientist in Joe C. Campbell Group, University of Virginia, Charlottesville. Her current research interests include high-power photodetectors and microwave photonics.

Qiugui Zhou received the B.S. degree in physics and M.S. degree in optics from University of Science and Technology of China, Hefei, Anhui, China, in 2001 and 2004, respectively. From 2004 to 2006, he was employed by BYD Company in China where he worked on LCDs. He received the Ph.D. degree in electrical engineering from the University of Virginia in 2011. His major research interests include optoelectronic devices with emphasis on photodiodes. He is currently working on optical communication components at JDS Uniphase in Milpitas, CA, USA.

Franklyn Quinlan's biography not available at the time of publication.

Tara M. Fortier's biography not available at the time of publication.

Scott A. Diddams is an experimental physicist working in the fields of precision spectroscopy and metrology, nonlinear optics, and ultrafast lasers. He received the Ph.D. degree from the University of New Mexico in 1996. He did postdoctroral work at JILA, University of Colorado, and since 2000 he has been a Staff Member and Project Leader at the National Institute of Standards and Technology (NIST). With his group and colleagues at NIST, he has developed optical frequency combs and pioneered their use in optical clocks, tests of fundamental physics, novel spectroscopy in the visible and mid-infrared, precision metrology, and ultralow noise frequency synthesis. He received the Department of Commerce gold and silver medals as well as the Presidential Early Career Award in Science and Engineering (PECASE) for his work on optical frequency combs. He is a Fellow of the Optical Society of America and the American Physical Society.

Andreas G. Steffan received the Dipl.-Ing. and Dipl.-Phys. degrees in electrical engineering and physics from the RWTH Aachen. In 2002, he received the Ph.D. degree from the University of Cambridge, England, and joined u^2t Photonics AG where he worked as a Project Manager on the development of transmitter, receivers, and test and measurement products, including modulators and pulsed laser sources. Since 2013, he has been the Leader of the R&D T&M and analog group at u^2t Photonics, working on novel device concepts for test and measurement and analog photonic applications.

Andreas Beling received the Dipl.-Phys. degree (M.S.) in physics from the University of Bonn, Germany, in 2000, and the Dr.-Ing. degree (Ph.D.) in electrical engineering from Technical University Berlin, Germany, in 2006. He was a Staff Scientist in the photonics division at the Heinrich-Hertz-Institut in Berlin in 2001–2006, a Research Associate in the Department of Electrical and Computer Engineering, at the University of Virginia in 2006–2008, and has 2 years of industry experience as a Project Manager working on optoelectronic receivers for high-speed fiber optic communication systems. He returned to University of Virginia in late 2010 as a Research Scientist and became Assistant Professor in the Department of Electrical and Computer Engineering at UVa in 2013. His research interests include photonic integration technologies and high-speed optoelectronic devices for optical communication systems and microwave photonics. He has authored or coauthored more than 100 technical papers, two book chapters, and three patents. He is a member of the IEEE Photonics Society and the Optical Society of America.

Joe C. Campbell received the B.S. degree in physics for the University of Texas at Austin in 1969, and the M.S. and Ph.D. degrees in physics from the University of Illinois at Urbana-Champaign Champaign, IL, USA, in 1971 and 1973, respectively. From 1974 to 1976, he was employed by Texas Instruments where he worked on integrated optics. In 1976, he joined the staff of AT&T Bell Laboratories in Holmdel, NJ, USA. In the Crawford Hill Laboratory, he worked on a variety of optoelectronic devices including semiconductor lasers, optical modulators, waveguide switches, photonic integrated circuits, and photodetectors with emphasis on high-speed avalanche photodiodes for high-bit-rate lightwave systems. In January of 1989, he joined the faculty of the University of Texas at Austin as a Professor of Electrical and Computer Engineering and Cockrell Family Regents Chair in Engineering. In January 2006, he moved to the University of Virginia in Charlottesville as the Lucian Carr Professor of Electrical and Computer Engineering. His technical area is photodetectors. At present, he is actively involved in single-photon-counting APDs, Si-based optoelectronics, high-speed low-noise avalanche photodiodes, high-power high-linearity photodiodes, ultraviolet analanche photodiodes, and solar cells. He has coauthored ten book chapters, 400 articles for refereed technical journals, and more than 400 conference presentations. He teaches graduate and undergraduate courses on lasers and optoelectronic components. In 2002, he was inducted into the National Academy of Engineering.